

# Enhanced Intracranial Microdialysis by Reduction of Traumatic Penetration Injury at the Probe Track

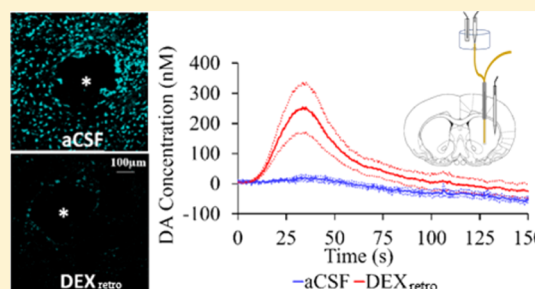
Erika L. Varner, Andrea Jaquins-Gerstl, and Adrian C. Michael\*

Department of Chemistry, University of Pittsburgh, 219 Parkman Avenue, Pittsburgh, Pennsylvania 15260, United States

## Supporting Information

**ABSTRACT:** Microdialysis provides deep insight into chemical neuroscience by enabling in vivo intracranial chemical monitoring. Nevertheless, implanting a microdialysis probe causes a traumatic penetration injury (TPI) of brain tissue at the probe track. The TPI, which is clearly documented by voltammetry and histochemical imaging, is a drawback because it perturbs the exact tissue from which the brain dialysate samples are derived. Our goal is to reduce, if not eventually eliminate, the TPI and its detrimental effects on neurochemical monitoring. Here, we demonstrate that combining a 5-day wait period after probe implantation with the continuous retrodialysis of a low-micromolar concentration of dexamethasone vastly reduces the TPI. Our approach to reducing the TPI reinstates normal evoked dopamine release activity in the tissue adjacent to the microdialysis probe, brings evoked dopamine release at the probe outlet into quantitative agreement with evoked dopamine release next to the probe, reinstates normal immunoreactivity for tyrosine hydroxylase and the dopamine transporter near the probe track, and greatly suppresses glial activation and scarring near the probe track. This reduction of the TPI and reinstatement of normal evoked dopamine release activity adjacent to the probe track appears to be due to dexamethasone's anti-inflammatory actions.

**KEYWORDS:** Microdialysis, dexamethasone, dopamine, voltammetry, penetration injury, retrodialysis



Microdialysis is a powerful and popular approach for intracranial chemical monitoring.<sup>1–4</sup> There are several reasons for this. The probes sample a broad array of interesting substances, limited mainly by the molecular weight cutoff of the dialysis membrane. Because the dialysate samples are free of macromolecules, blood, and cellular debris, they are suitable for near real-time analysis by online methods without further sample preparation. Brain dialysate is compatible with a variety of high-performance analytical methods, including HPLC, capillary electrophoresis, and mass spectrometry. Recent enhancements of such methods have produced substantial gains in temporal resolution.<sup>5–7</sup> The power and utility of microdialysis has spawned a vast literature on intracranial monitoring in awake, freely moving animals and in human patients with brain injury.<sup>1–8</sup>

Nevertheless, implanting a microdialysis probe causes a traumatic penetration injury (TPI) to brain tissue that triggers ischemia, opens the blood–brain barrier, activates astrocytes and microglia, damages neurons, axons and terminals, and leads to scar formation at the probe track.<sup>9–15</sup> This scenario is not unique to microdialysis, as TPI also confronts brain–machine interfaces.<sup>16,17</sup> The TPI significantly perturbs the neurochemistry of the tissue from which the dialysate samples are obtained<sup>14,15,18,19</sup> and contributes to the loss in probe patency over time following implantation.<sup>20–24</sup> Thus, our objective is to reduce, if not eventually eliminate, the TPI and its deleterious effects on neurochemical monitoring.

Herein, we show that combining a 5-day postimplantation wait period with the continuous retrodialysis of a low-micromolar concentration of dexamethasone vastly reduces both the voltammetric and histological signs of TPI. Dexamethasone (DEX) is a glucocorticoid anti-inflammatory agent. We have previously documented that continuous DEX retrodialysis (DEX<sub>retro</sub>) diminishes TPI at 4 and 24 h after probe implantation.<sup>14,15</sup> However, we now show that at 5-days after probe implantation DEX<sub>retro</sub> reinstates normal evoked dopamine (DA) release activity in the tissue adjacent to the probe, facilitates robust detection of evoked DA release at the probe outlet (i.e., without the aid of a DA uptake inhibitor), establishes quantitative agreement between evoked DA measured simultaneously at the probe outlet and in the tissue next to the probe, reinstates normal immunoreactivity for tyrosine hydroxylase (TH) and the dopamine transporter (DAT) near the probe, and prevents glial scarring at the probe track. Our findings support the conclusion that the beneficial effects of DEX in this application may be attributed to its actions as an anti-inflammatory agent.

## RESULTS AND DISCUSSION

**Experimental Design.** Microdialysis probes were implanted unilaterally into the striatum of rats and perfused

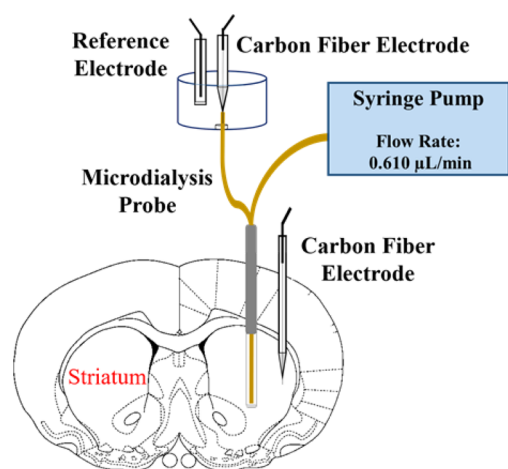
Received: December 14, 2015

Accepted: March 22, 2016

Published: March 22, 2016

continuously for 5 days with or without DEX<sub>retro</sub>. As before,<sup>13</sup> we perfused the probes with 10  $\mu\text{M}$  DEX for the first 24 h after probe implantation and then switched to 2  $\mu\text{M}$  DEX thereafter. Five days after probe implantation, the rats were reanesthetized and returned to a stereotaxic frame, where they remained for the duration of the measurements reported below. A stimulating electrode was placed in the medial forebrain bundle ipsilateral to the microdialysis probe, and a carbon fiber electrode was placed in the striatum at a location 1.0 or 1.5 mm from the microdialysis probe, as specified below. The outlet capillary of the microdialysis probe was threaded into a detection chamber and interfaced to a second carbon fiber electrode (Scheme 1). This setup permits evoked DA

#### Scheme 1<sup>a</sup>



<sup>a</sup>Five days after implanting a microdialysis probe into the striatum, a carbon fiber electrode was placed 1.5 mm from the probe. The outlet of the microdialysis probe was threaded into a detection chamber and interfaced to a second carbon fiber electrode. This arrangement allows simultaneous recordings of evoked DA release at the probe outlet and in the tissue next to the probe.

responses to be recorded by fast scan cyclic voltammetry (FSCV) simultaneously at the probe outlet and in the tissue adjacent to the probe. The stimulations were applied for 25 s at 45 Hz unless noted otherwise. The 25-s stimulus duration was selected, based on prior work, to match the response time of the microdialysis probes (see Figure 6 of ref 25).

In the figures that follow, the time axes for responses recorded at the probe outlet are corrected to account for the time required for the dialysate to travel the length of the outlet capillary. DA concentrations recorded at the probe outlet have not been corrected for probe recovery. DEX<sub>retro</sub> had no significant effect on evoked DA responses recorded in the striatal tissue 1.5 mm from the microdialysis probes (Figure S1).

#### Evoked DA Responses Recorded at the Probe Outlet.

Figure 1 compares evoked DA responses recorded at the probe outlet 5-days after implantation with (red) or without (blue) continuous DEX<sub>retro</sub>. Without DEX<sub>retro</sub> there was no response (0 responses from 6 rats). With DEX<sub>retro</sub>, however, the response was both robust and reproducible (6 responses from 6 rats).

In our view, the evoked response recorded at the probe outlet after 5 days of DEX<sub>retro</sub> (Figure 1, red) represents a major step forward in our efforts to reduce, if not eventually eliminate, the TPI. During our prior studies at 4 and 24 h after probe

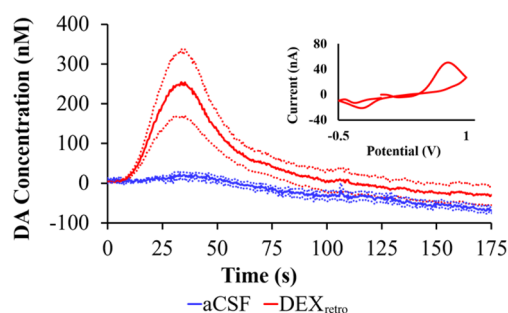


**Figure 1.** Evoked DA responses (mean  $\pm$  SEM,  $n = 6$  per group) recorded at the outlet of microdialysis probes 5 days after implantation. Without DEX<sub>retro</sub> (blue) the stimulus evoked no response. With DEX<sub>retro</sub> (red), the stimulus evoked clear and reproducible responses. Inset: the average background-subtracted cyclic voltammogram obtained with DEX<sub>retro</sub>, showing the expected DA oxidation and reduction peaks.

implantation,<sup>15,23,25,26</sup> we have never observed a pre-nomifensine response by voltammetry at the probe outlet, either with or without DEX<sub>retro</sub>. The requirement for uptake inhibition stems from the TPI, which abolishes evoked DA release in the tissue adjacent to the probe.<sup>14,15,18,19</sup> Figure 1 is the first of several observations reported herein indicating a vast reduction in the TPI by the combination of DEX retrodialysis and a sufficient postimplantation wait interval.

To permit comparisons with evoked responses previously measured at 4 and 24 h after probe implantation,<sup>15</sup> we recorded additional responses at the probe outlet after treating rats first with nomifensine (20 mg/kg i.p.), a DAT inhibitor, and then with raclopride (2 mg/kg i.p.), a dopamine D2 receptor antagonist (Figure 2A,B). Figure 2C and D summarizes the maximum amplitude and the area under the curve (AUC) of the evoked responses. We performed the AUC analysis because the temporal profile of the outlet responses was somewhat altered after the 5-day wait interval (see Figures S2 and S3). The amplitude of the pre-nomifensine response with DEX<sub>retro</sub> is significant (one-tailed  $t$  test). DEX<sub>retro</sub> significantly increased the post-nomifensine and post-nomifensine/raclopride amplitudes and AUCs (ANOVA; details are in the figure legend).

Without DEX<sub>retro</sub>, evoked responses at the outlet of probes implanted in animals treated with nomifensine and then with raclopride exhibited significant decreases in amplitude and AUC between 4 and 24 h after implantation and showed no tendency to rebound after 5 days (Figure 3). However, with DEX<sub>retro</sub> there were no such declines (Figure 3). Instead, DEX<sub>retro</sub> stabilized the postdrug responses, which exhibited only minor differences among the 4 h, 24 h, and 5 day time points. It is important to emphasize that different groups of animals were used for each time point and for each condition (aCSF and DEX).

**Comparison of Outlet and In Vivo Responses.** Figure 4 compares the amplitudes of responses recorded at the probe outlet after 5 days of continuous DEX<sub>retro</sub> (Figure 4A) to the amplitudes of in vivo responses recorded in the tissue adjacent to the probe (the probe–electrode separation was 1.5 mm, Figure 4B). Responses at the outlet are in the 200–700 nM range, whereas the in vivo responses are in the 5–20  $\mu\text{M}$  range. Thus, the in vivo recovery ratio of evoked DA is on the order of 5%.

Because of our new ability to record outlet responses without the aid of nomifensine, it is now possible to report the

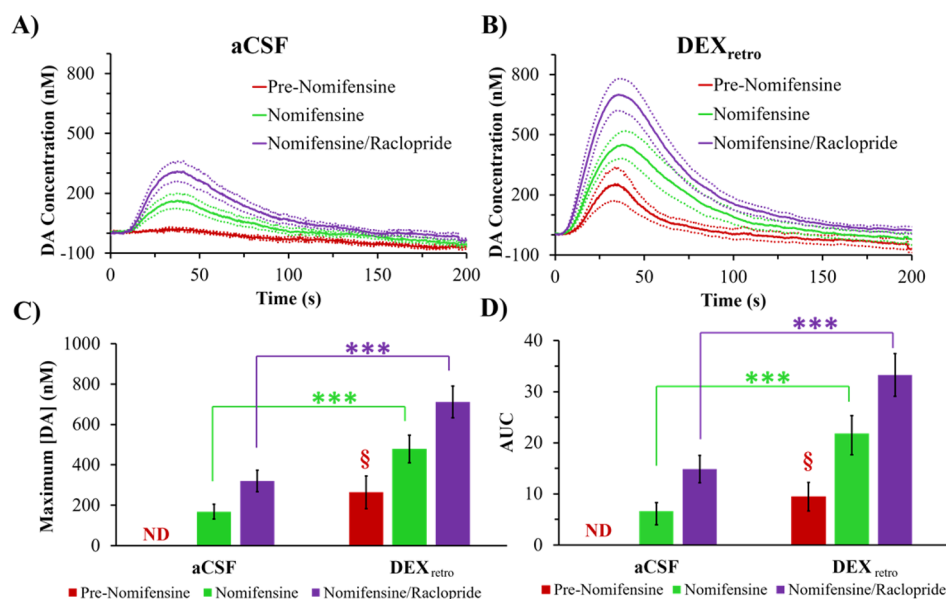


**Figure 2.** Evoked DA responses (mean  $\pm$  SEM,  $n = 6$  per group) measured at the outlet of microdialysis probes perfused with (A) aCSF or (B) DEX. DA was measured before nomifensine (red), after nomifensine (green), and then again after raclopride (purple). The amplitudes and AUCs are analyzed in C and D, respectively (ND = not detected). The 5 day DEX<sub>retro</sub> pre-nomifensine responses are significant when compared to zero (amplitude,  $t(5) = 3.27$ ; AUC,  $t(5) = 3.40$ ; one-tailed  $t$  test; § =  $p < 0.05$ ). The amplitude and AUC results underwent 2-way ANOVA with treatment (aCSF, DEX) and drug (nomifensine and nomifensine/raclopride; repeated measurements) as factors. (C) Treatment ( $F(1,10) = 19.93$ ,  $p < 0.005$ ) and drug ( $F(1,10) = 26.96$ ,  $p < 0.001$ ) are significant factors: no significant interaction. (D) Treatment ( $F(1,10) = 18.25$ ,  $p < 0.005$ ) and drug ( $F(1,10) = 21.96$ ,  $p < 0.001$ ) are significant factors: no significant interaction. Asterisks report posthoc pairwise comparisons. \*\*\* $p < 0.005$ .

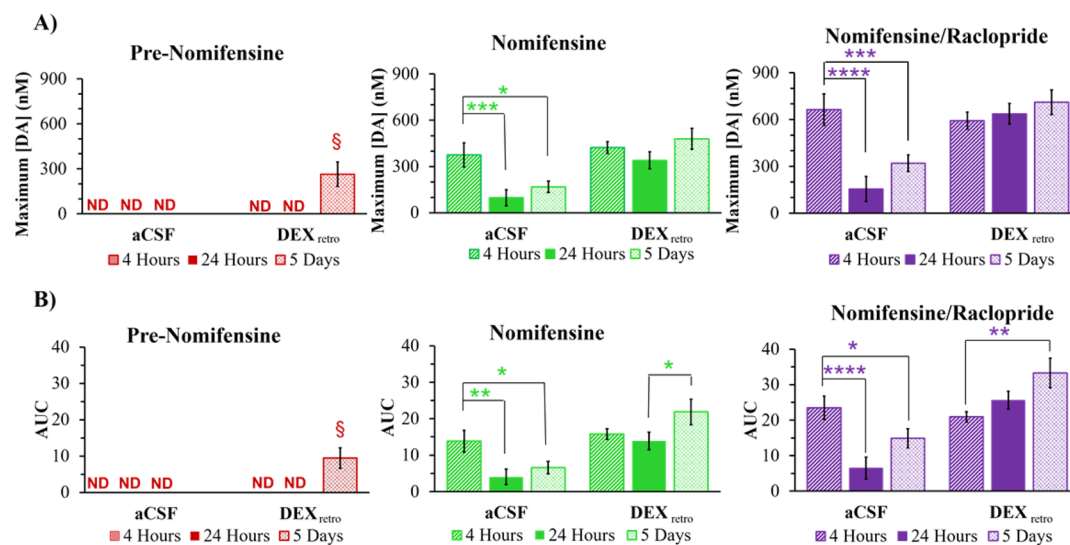


**Figure 3.** (A) Amplitude and (B) AUC (mean  $\pm$  SEM,  $n = 6$  per group) of evoked DA responses detected at the probe outlet (ND = not detected). The data at 4 h, 24 h, and 5 days are from separate groups of rats. The data at 4 and 24 h are from a prior study.<sup>15</sup> The 5 day DEX<sub>retro</sub> pre-nomifensine responses are statistically significant compared to zero (amplitude,  $t(5) = 3.27$ ; AUC,  $t(5) = 3.40$ ; one-tailed  $t$  test, § =  $p < 0.05$ ). Statistical analysis of the nomifensine and nomifensine/raclopride panels was by three-way ANOVA with time (4 h, 24 h, and 5 days), treatment (aCSF and DEX), and drug (nomifensine and nomifensine/raclopride; repeated measurements). Time (amp  $F(2,30) = 5.69$ ,  $p < 0.01$ , AUC  $F(2,30) = 4.66$ ,  $p < 0.05$ ), treatment (amp  $F(1,30) = 21.8$ ,  $p < 0.001$ , AUC  $F(1,30) = 28.1$ ,  $p < 0.001$ ), and drug (amp  $F(1,30) = 100$ ,  $p < 0.001$ , AUC  $F(1,30) = 57.2$ ,  $p < 0.001$ ) are significant factors. Interactions are significant. Asterisks indicate posthoc pairwise comparisons. \* $p < 0.05$ , \*\* $p < 0.01$ , \*\*\* $p < 0.005$ , and \*\*\*\* $p < 0.001$ .

amplitude of both the outlet and in vivo responses normalized with respect to their pre-nomifensine amplitudes (Figure 4C). We found no significant differences between the normalized outlet and normalized in vivo responses (statistical details are in the figure legend). Thus, Figure 4C indicates essentially perfect quantitative agreement between the outlet and in vivo responses.

Figure 4C represents the first occasion upon which we have been able to report near-perfect quantitative agreement between evoked responses recorded at the outlet of probes and in the tissue adjacent to the probes. Prior studies have consistently found that uptake inhibition increases the in vivo recovery of DA.<sup>7,15,18,23,25–29</sup> On theoretical grounds, we suggested that the impact of DAT inhibition on the in vivo

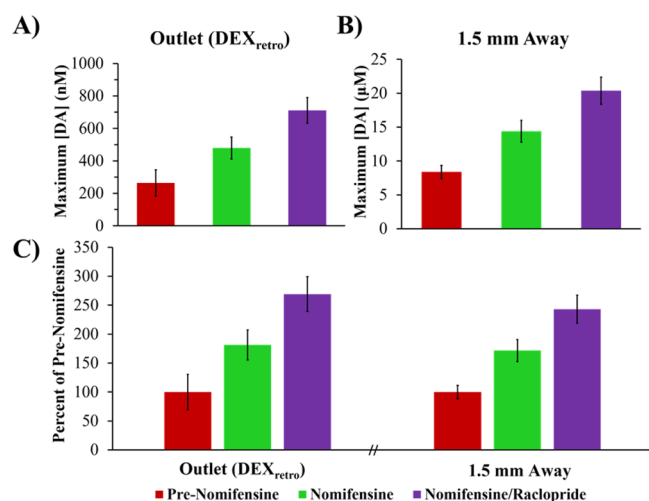


**Figure 4.** Evoked DA (mean  $\pm$  SEM) measured (A) at the probe outlet after 5 days of DEX<sub>etro</sub> ( $n = 6$ , data from Figure 2C) and (B) directly in the striatal tissue ( $n = 18$ ; Figure S1 data combined). (C) Response amplitudes normalized with respect to the pre-nomifensine amplitude. Statistical analysis was by a two-way ANOVA for location (outlet, tissue) and drug (nomifensine, nomifensine/raclopride; repeated measurements). Only the drug was a significant factor ( $F(1,22) = 16.99$ ,  $p < 0.001$ ): neither location nor interaction were significant.

recovery of DA is indicative of the presence of a zone of disrupted tissue adjacent to the probe wherein DA uptake exceeds DA release.<sup>26,30,31</sup> Figure 4 strongly suggests that this zone of disrupted tissue is no longer present under the conditions of these measurements, strongly suggesting that the combination of a 5-day postimplantation interval with continuous retrodialysis of DEX vastly reduces the TPI.

**In Vivo Voltammetry Next to the Probe.** A second series of experiments was performed to directly assess the impact of DEX<sub>etro</sub> on evoked DA release activity in the tissue surrounding the probe. Five days after probe implantation, evoked DA responses were recorded in vivo with two carbon fiber microelectrodes. As in a prior study,<sup>15</sup> one electrode was placed 1 mm from the probe, and the other was placed 100  $\mu$ m from the probe (Figure 5A and C). Without DEX<sub>etro</sub> the evoked responses 100  $\mu$ m from the probe were either abolished or significantly reduced (Figure S4), consistent with prior observations at 4 and 24 h after implantation.<sup>15</sup> However, with DEX<sub>etro</sub> there were no significant differences between the response amplitudes measured 1 mm and 100  $\mu$ m from the probe (Figure 5B).

In our prior study at 4 and 24 h after probe implantation,<sup>15</sup> evoked responses in close proximity to probes perfused with DEX (probe–electrode separation of 100  $\mu$ m) were detectable but significantly lower in amplitude than normal. Thus, Figure 5 clearly indicates that combining a 5-day postimplantation wait time with continuous DEX<sub>etro</sub> leads to a reinstatement of normal evoked DA activity in close proximity to the probe.

**DA Kinetic Analysis.** Additional responses were recorded 1 mm and 100  $\mu$ m from the probe using a 3-s stimulus delivered at 60 Hz. The responses underwent kinetic analysis with the numerical model of Walters et al.<sup>32</sup> The model provides excellent fits to responses recorded 100  $\mu$ m away with DEX<sub>etro</sub> and to responses 1 mm away either with or without DEX<sub>etro</sub> (Figure 6). Moreover, there were no significant differences between the kinetic parameters providing best fits to these responses (Table S1). Thus, after 5 days of continuous DEX<sub>etro</sub>, we detect no significant alterations in the kinetics of DA release, uptake, or transport in close proximity to the microdialysis probes.

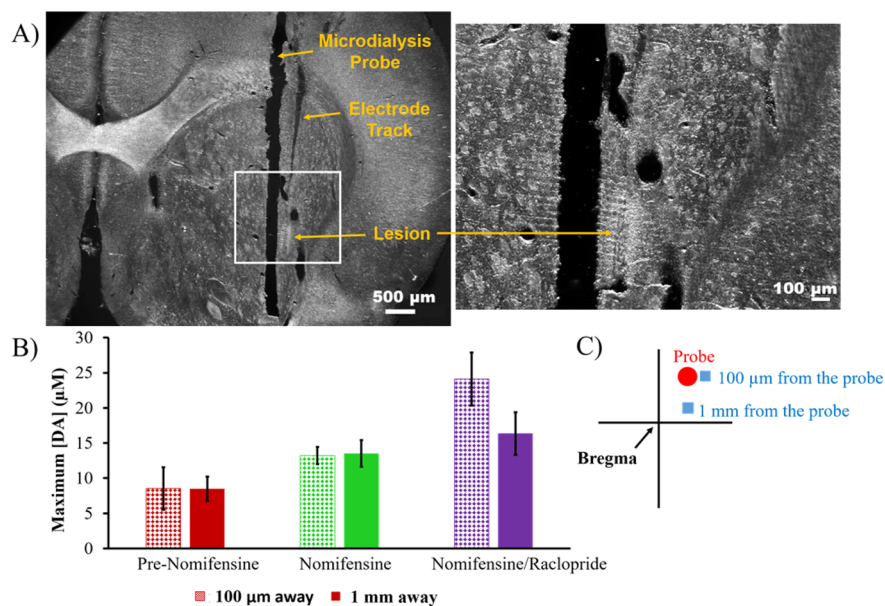


**Figure 5.** (A) Electrolytic lesion confirmed the placement of a carbon fiber electrode 100  $\mu$ m from the microdialysis probe by applying a current of 20  $\mu$ A for 5 s to the electrode. The white box in the left image is magnified on the right. Scale bars are 500  $\mu$ m (left) and 100  $\mu$ m (right). (B) Evoked release (mean  $\pm$  SEM,  $n = 4$  per group) measured 100  $\mu$ m (pattern) and 1 mm (solid) away from the probe after 5 days of DEX<sub>etro</sub> (responses in Figure S4). Statistical analysis was by two-way ANOVA for the drug (pre-nomifensine, nomifensine, and nomifensine/raclopride; repeated measurements) and location (100  $\mu$ m, 1 mm). The drug was significant ( $F(1,6) = 23.02$ ,  $p < 0.005$ ), while the location and the interaction were not significant factors. (C) Schematic of voltammetry next to the probe with the electrodes represented by blue boxes and the probe by a red circle. The adjacent electrode was implanted at a 5° angle to allow the tip of the electrode to be placed 100  $\mu$ m from the probe.

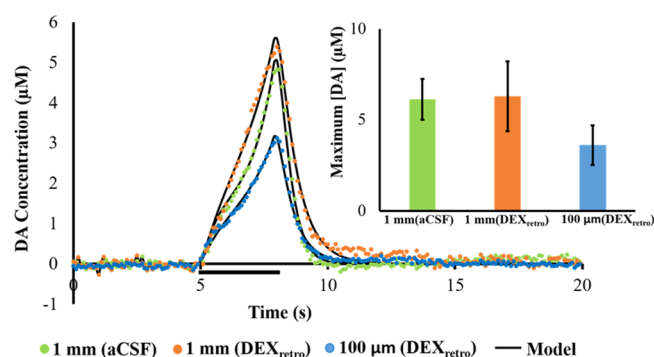


**Figure 6.** Evoked release (mean,  $n = 4$  per group) measured 1 mm away without (green) and with (orange) DEX<sub>etro</sub> and 100  $\mu\text{m}$  from the probe with DEX<sub>etro</sub> (blue): error bars are omitted for clarity. The stimulus in this case was for 3 s (marked by the horizontal black bar) at 60 Hz. The black lines report the average of the kinetic fits to each individual response. The average values of the kinetic parameters (see Table S1) exhibited no significant differences (multivariate ANOVA, Pillai's Trace). The inset shows the response amplitudes, which are not statistically different (one-way ANOVA).

**Immunohistochemistry.** Horizontal tissue sections (35  $\mu\text{m}$  thick) containing the probe tracks were immunolabeled for TH and DAT, two widely accepted markers of DA terminals (Figures S5 and S6), and for ED-1, a marker of microglia and macrophages.<sup>33,34</sup> The images were quantified by the pixel counting routines built into Metamorph (see Methods).

Images of TH and DAT immunoreactivity in tissues surrounding the tracks of probes perfused for 5 days with or without DEX<sub>etro</sub> were indistinguishable from each other and from images of nonimplanted control tissue (Figure 7). All images exhibited extensive immunoreactivity except in locations corresponding to myelinated axon bundles, blood vessels, and the probe tracks: all such features were clearly visible in DIC images of the same tissues. Quantitative image analysis produced no significant differences among these images (ANOVA details are in the figure legend). Images at higher magnification (40, 60, and 100 $\times$ ) indicate punctate TH labeling up to the very edge of the probe tracks (Figure S7).

These findings stand in stark contrast to our observations of marked disruptions of TH immunoreactivity near probe tracks at 4 and 24 h after implantation, especially when DEX<sub>etro</sub> was absent.<sup>14,15</sup> The reinstatement of normal TH and DAT immunoreactivity appears to be in excellent agreement with

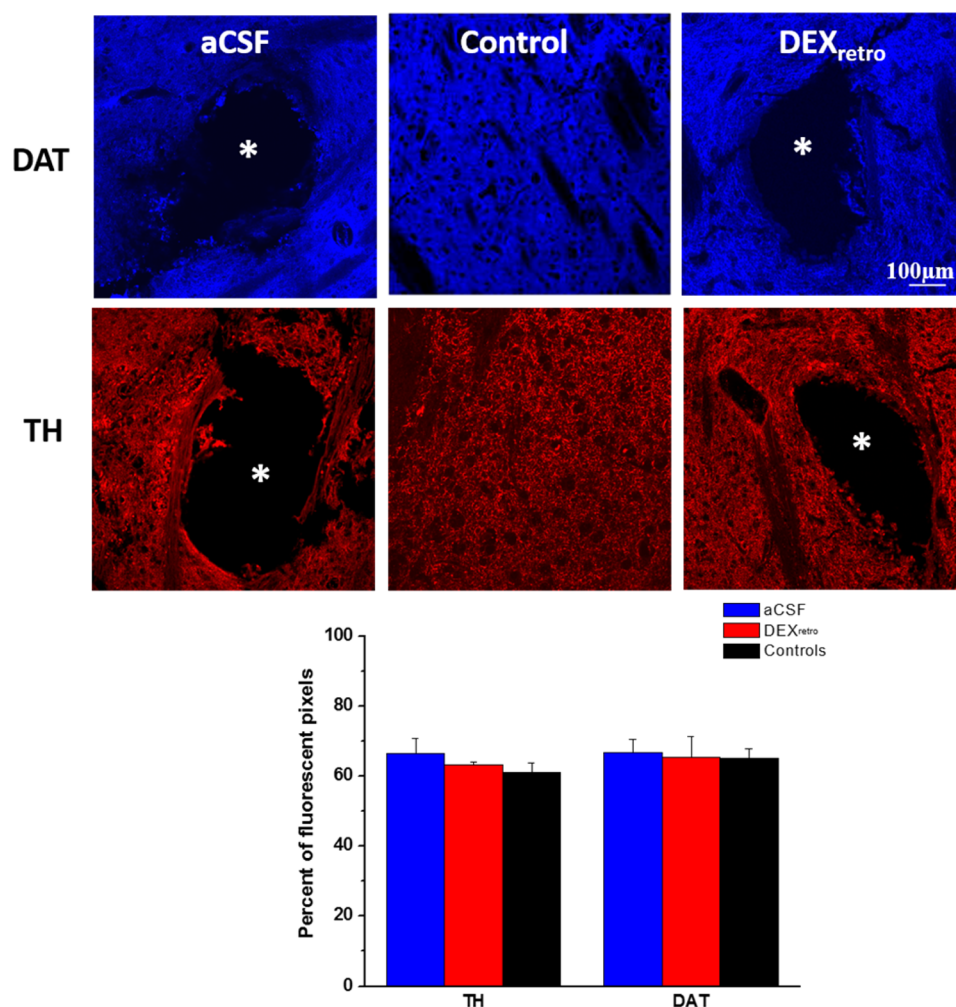


**Figure 7.** DAT (blue) and TH (red) immunoreactivity in tissue sections containing tracks of probes perfused without (left) and with (right) DEX<sub>etro</sub> for 5 days and in sections of nonimplanted control tissue (center). Asterisks mark the center of the probe tracks. Scale bar = 100  $\mu\text{m}$ . The bottom graph shows the quantification of the fluorescent pixels for each marker: the probe tracks were excluded from the regions of interest. In a 2-way ANOVA of treatment (aCSF, DEX, and control) and antibody (TH and DAT), neither the treatment nor the antibody was a significant factor.

the reinstatement of evoked DA activity in close proximity to the probes (Figures 1–5). However, images of TH and DAT immunoreactivity near probes perfused without DEX also appear similarly normal, which comes as a surprise because evoked DA release adjacent to and at the outlet of these probes show major disruptions (Figure 1 and S4). Thus, the ability of 5 days of DEX<sub>retro</sub> to reinstate normal evoked DA release activity cannot be attributed solely to the reinstatement of normal TH and DAT immunoreactivity.

During previous work, we showed that 5 days of DEX<sub>retro</sub> is highly effective at suppressing the activation of astrocytes and preventing the formation of a glial scar at the probe track<sup>13</sup> (see also Figure S8). Here, we document that DEX<sub>retro</sub> is likewise highly effective at suppressing the activation of microglia (Figure 8). Thus, our histochemical findings suggest that the

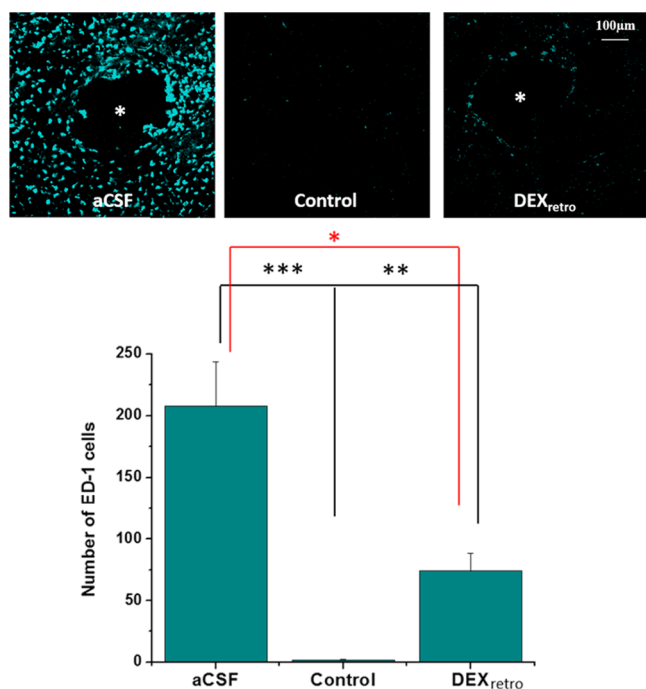


**Figure 8.** Immunoreactivity for ED-1 in sections containing the tracks of probes without (left) or with DEX<sub>retro</sub> (right) and sections from nonimplanted control tissue (center) (asterisks represent the center of the probe track, scale bar = 100  $\mu$ m). The bottom graph compares counts of ED-1 positive cells in area matched sections of aCSF, DEX<sub>retro</sub>, and control tissue. Statistical analysis was by one-way ANOVA,  $F(2,22) = 21.560$ ,  $p < 0.001$ . Asterisks report the posthoc tests (Games–Howell). \* $p < 0.05$ , \*\* $p < 0.01$ , and \*\*\* $p < 0.005$ .

reinstatement of normal TH and DAT immunoreactivity in close proximity to the probes is necessary but not sufficient for reinstatement of evoked DA release activity, as suppression of gliosis and scar formation is also critical.

## CONCLUSIONS

Our findings confirm that combining a 5-day postimplantation wait period with concurrent and continuous DEX<sub>retro</sub> vastly reduces the TPI of the brain tissue at the microdialysis probe track. This enables the recording of robust and reproducible evoked DA responses at the probe outlet, which can be attributed to a reinstatement of normal evoked DA activity in the tissues in close proximity to the probes. Furthermore, the reinstatement of normal evoked DA activity adjacent to the

probes blocked nomifensine's ability to alter the in vivo microdialysis recovery of DA, a phenomenon previously attributed to a zone of disrupted tissue at the probe track.<sup>26,30,31</sup> Overall, combining a 5-day postimplant interval with DEX<sub>retro</sub> brings evoked DA responses at the probe outlet into excellent quantitative agreement with in vivo responses. In our line of investigation into these matters, this is the first occasion upon which we have observed such excellent agreement. The efficacy of DEX in this work appears to be due to its anti-inflammatory actions, as markers of DA terminals appear normal upon histochemical examination after 5 days regardless of whether DEX<sub>retro</sub> was performed. Thus, the reinstatement of normal TH and DAT immunoreactivity, accepted markers of DA terminals, at the probe track is necessary but not sufficient for the reinstatement of normal evoked DA release activity, as suppression of gliosis and scarring is also critical.

Our conclusion that the postimplantation wait period is an important contributor to the reinstatement of DA function in close proximity to the probe concurs with the work of Di Chiara and colleagues.<sup>35–37</sup> In their work, histology after several weeks of repetitive probe insertions through a guide cannula shows the presence of TH-positive varicosities and no signs of necrosis.<sup>35–37</sup> This concurs with our finding (Figure 7) that DA terminals appear normal as early as 5 days after probe implantation. However, our findings show that gliosis is also an important consideration.

The choice of dexamethasone as an anti-inflammatory agent raises some potentially contentious issues as steroids have their own neurochemical actions.<sup>38</sup> During this work, we found no evidence that dexamethasone altered evoked DA release, which is consistent with a body of literature indicating that DA systems are not highly sensitive to steroids.<sup>39–43</sup> Thus, the effects of DEX described above appear to reflect anti-inflammatory rather than neurochemical mechanisms. However, DEX might prove unsuitable in some microdialysis investigations of other neurochemical systems that exhibit greater sensitivity to steroids. In this light, it is relevant to mention that alternatives to DEX are available, including nonsteroidal anti-inflammatory drugs. It is also worth mentioning that retrodialysis, even over extended time periods, involves truly minuscule quantities of drug: the total amount of dexamethasone delivered via retrodialysis during the experiments reported here is less 20 nanomoles. While alternative anti-inflammatory strategies (agent, dose, duration, etc.) remain to be explored, we believe that this work clearly establishes the overall principle of anti-inflammatory enhanced microdialysis.

## METHODS

All use of animals was approved by the University of Pittsburgh Institutional Animal Care and Use Committee. Some of the methods and procedures employed for the present study have been previously described.<sup>7,15</sup>

**Reagents and Solutions.** All solutions were prepared with ultrapure water (Nanopure; Barnstead, Dubuque, IA). Artificial cerebrospinal fluid (aCSF: 142 mM NaCl, 1.2 mM CaCl<sub>2</sub>, 2.7 mM KCl, 1.0 mM MgCl<sub>2</sub>, and 2.0 mM NaH<sub>2</sub>PO<sub>4</sub>, pH 7.4) was used for voltammetric DA calibration and as the perfusion fluid of the microdialysis probe. Dexamethasone sodium phosphate (APP Pharmaceuticals LLC, Schaumburg, IL) was diluted in aCSF. The perfusion fluids for microdialysis were filtered with Nalgene sterile filter units (Fisher, Pittsburgh, PA; PES 0.2  $\mu$ m pores). Nomifensine maleate and *S*(-)-raclopride (+)-tartrate (Sigma-Aldrich, St. Louis, MO) were dissolved in phosphate-buffered saline (PBS: 137 mM

NaCl, 2.7 mM KCl, 1.47 mM  $\text{KH}_2\text{PO}_4$ , and 10 mM  $\text{Na}_2\text{HPO}_4$ , pH 7.4) and administered at 20 mg/kg and 2 mg/kg (i.p.), respectively. DA (Sigma-Aldrich, St. Louis, MO) standards were prepared in  $\text{N}_2$ -purged aCSF for electrode calibration.

**Microdialysis Probes and DEX<sub>retro</sub>.** Concentric-style microdialysis probes (300  $\mu\text{m}$  in diameter, 4 mm membrane length) were built in-house (13 kDa MWCO Spectra/Por hollow fiber, Spectrum Laboratories Inc. Rancho, Dominguez, CA). Fused silica capillaries (75  $\mu\text{m}$  I.D., 150  $\mu\text{m}$  O.D., Polymicro Technologies, Phoenix, AZ) were used for the inlet and outlet lines. The probe inlet was connected to a syringe pump (Harvard Apparatus, Holliston, MA) running at 0.610  $\mu\text{L}/\text{min}$ . The outlet capillary was 10 cm long. Prior to use, the probes were soaked in 70% ethanol and then immersed in and flushed with filtered perfusion fluid for several hours before implantation (aCSF or aCSF with DEX). During procedures involving DEX<sub>retro</sub>, the probe was perfused first with 10  $\mu\text{M}$  DEX for 24 h and thereafter with 2  $\mu\text{M}$  DEX, as previously described.<sup>13</sup> When DEX was used, it was added to the perfusion fluid prior to probe implantation.

**Voltammetry.** Carbon fiber electrodes were constructed by placing a single carbon fiber (7  $\mu\text{m}$  diameter, T650, Cytec Carbon Fibers LLC., Piedmont, SC) in a borosilicate capillary (0.58 mm I.D., 1.0 mm O.D., Sutter Instruments, Novato, CA), pulling the capillary to a fine tip (Narishing Tokyo, Japan), sealing the tip with a low viscosity epoxy (Spurr Epoxy, Polysciences Inc., Warrington, PA), and trimming the exposed fiber to 400 or 800  $\mu\text{m}$  for in vivo and outlet recordings, respectively. FSCV was performed with a potentiostat (EI-400, Enscan Instruments, Bloomington, IN) and CV Tarheel software (version 4.3, Michael Heien, University of Arizona, Tucson AZ). The waveform began at the rest potential of 0 V, scanned to +1.0 V, then to -0.5 V, and back to the rest potential at 400 V/s: potentials are vs Ag/AgCl. Scans were performed at 2.5 Hz during the 25-s stimulations and 10 Hz for the 3-s stimulations. The 800  $\mu\text{m}$  outlet electrodes were pretreated (0–2 at 200 V/s for 3 s) 10 min before each stimulus or calibration procedure. This pretreatment improves sensitivity but also causes some drift in the FSCV background signal, which is noticeable at low DA concentrations (~20–30 nM).<sup>25</sup> To minimize the drift, the pretreatment was followed by application of the FSCV waveform at 60 Hz for 120 s.

**Voltammetry at the Microdialysis Probe Outlet.** The outlet capillary was passed through the floor of a Plexiglas electrochemical cell. The microelectrode for FSCV at the outlet was inserted into the capillary end with a miniature micromanipulator (Fine Science Tools, Foster City, CA). To confirm the performance of the probe and the electrode, calibration was performed by exposing the probe to a 10  $\mu\text{M}$  DA solution for 30 s prior to animal use.

**Surgical and Stimulation Procedures.** Prior to surgery, rats (male Sprague–Dawley, 250–350g, Charles River, Raleigh, NC) were acclimated overnight to a Ratum Microdialysis Bowl (MD-1404, BASI, West Lafayette, IN). The next day, the rats were anesthetized with isoflurane (0.5% by volume  $\text{O}_2$ ) and implanted with microdialysis probes following aseptic stereotaxic surgical technique. Using flat skull coordinates,<sup>44</sup> the probes were slowly lowered into the striatum (1.6 mm anterior, 2.5 mm lateral from bregma, and 7.0 mm below the dura) at 5  $\mu\text{m}/\text{s}$  using a micropositioner (David Kopf Instruments, Tujunga, CA). Probes were secured with bone screws and acrylic cement and the incision was closed with sutures (there was no guide cannula). Anesthesia was removed and animals were returned to the Ratum system and given free access to food and water.

After 5 days, the rats were reanesthetized and returned to the stereotaxic frame, where they remained for the duration of all procedures. A reference electrode was contacted to the brain surface with a salt bridge, a carbon fiber microelectrode was inserted into the striatum 1.5 mm away from the probe (0.45 mm anterior to bregma, 3.5 mm lateral from bregma, and 5.0 mm below dura), and a bipolar stimulating electrode was lowered into the medial forebrain bundle ipsilateral to the probe and carbon fiber microelectrode (4.3 mm posterior from bregma, 1.2 mm lateral from midline, and 7.2 mm below the dura). The stimulus waveform was a biphasic, square wave with constant current pulses (300  $\mu\text{A}$  pulse height and 4 ms pulse width). The waveform was delivered for 25 s at 45 Hz or 3 s at 60 Hz.

Nomifensine and raclopride were sequentially administered (i.p.), and evoked DA responses were recorded 20 min after each drug administration. A second series of evoked responses were recorded in the tissue next to the probes with carbon fiber electrodes placed 1 mm and 100  $\mu\text{m}$  from the probes, as previously described.<sup>15</sup>

At the end of the experiment, while the rats were deeply anesthetized, the locations of the carbon fiber electrodes were marked with a current lesion (20  $\mu\text{A}$  for 5 s) just before the rats were perfused through the heart to preserve the brain for subsequent analysis.<sup>13</sup>

**Area under the Curve (AUC) Analysis.** The responses measured at the probe outlet (black line, Figure S3) underwent an AUC analysis. If the response exhibited baseline drift, as discussed above, the drift was measured and subtracted (purple line, Figure S3). Next, we applied the “hang-up” correction described elsewhere<sup>32</sup> (green line, Figure S3). The AUC was determined with MATLAB’s trapezoidal integration function in units of micromolar and seconds.

**Immunohistochemistry.** Horizontal tissue sections (35  $\mu\text{m}$  thick) were prepared in a cryostat and stored at -20 °C until further use. Tissue sections were hydrated in PBS, blocked with 20% normal goat serum, 1% bovine serum albumin, and 0.3% Triton X (Sigma) in PBS (2.5 h). Sections were then incubated with primary antibodies for TH (1.5:1000, Millipore, Temecula, CA), DAT (1:400, Synaptic Systems, Göttingen, Germany), or ED-1 (for activated microglia/macrophages, CD68, 1:100, AbD Serotec, Raleigh, NC). Secondary antibodies were goat anti-rabbit IgG, CY3 (Invitrogen, USA) for TH, while ED-1 and DAT used goat anti-rabbit IgG Cy5 (Invitrogen, USA). Secondary antibodies were diluted 1:1000 in blocking solution. Sections were rinsed in PBS (3 × 5 min) and coverslips added with Fluoromount-G (Southern Biotechnology Associates, Birmingham, Alabama).

**Fluorescence Microscopy and Image Analysis.** Fluorescence microscopy (Olympus BX61, Olympus; Melville, NY) was performed with a 20, 40, 60, and 100× objective using appropriate filter sets (Chroma Technology; Rockingham, VT). The Metamorph/Fluor 7.1 software package (Universal Imaging Corporation; Molecular Devices) was used to collect, threshold, analyze, and quantify the images. The numbers of ED-1 positive cells in the section of the tissue surrounding the microdialysis track were counted. The number of fluorescent pixels in the TH and DAT images was expressed as a percent of pixels in the region of interest, which excluded the probe track. A minimum of 3 animals per group with 3 slices per brain were used for the statistical analysis.

**Statistics.** IBM Statistical Package for the Social Sciences (SPSS) 22 software was used for all statistical analysis. For ANOVA, SPSS was used to check for parameter normality and equality of variance. For statistical significance,  $p < 0.05$  was used for all tests.

## ■ ASSOCIATED CONTENT

### 📄 Supporting Information

The Supporting Information is available free of charge on the ACS Publications website at DOI: 10.1021/acscchemneuro.5b00331.

Additional information as noted in the text (PDF)

## ■ AUTHOR INFORMATION

### Corresponding Author

\*Phone: 412-624-8560. E-mail: amichael@pitt.edu.

### Author Contributions

E.L.V. collected and analyzed all of the voltammetry data at the outlet and next to the microdialysis probe. A.J.G. performed the immunohistochemical staining and imaging of the tissue for TH, DAT, ED-1, and GFAP. A.C.M. provided guidance in the experimental design and analysis. All authors co-wrote the manuscript.

## Funding

This work was funded by the NIH (NS 081744) and by the NSF Graduate Research Fellowship Program (to E.L.V.; 1247842).

## Notes

The authors declare no competing financial interest.

## ABBREVIATIONS

TPI, traumatic penetration injury; DA, dopamine; DEX, dexamethasone; DEX<sub>retro</sub>, retrodialysis of dexamethasone; FSCV, fast scan cyclic voltammetry; aCSF, artificial cerebrospinal fluid; AUC, area under the curve; TH, tyrosine hydroxylase; DAT, dopamine transporter; DIC, differential interference contrast; GFAP, glial fibrillary acidic protein

## REFERENCES

- (1) Robinson, T. E., Justice, J. B., Eds. (1991) *Techniques in the Behavioral and Neural Sciences*, Vol. 7: Microdialysis in the Neurosciences, Elsevier, Amsterdam.
- (2) Davies, M. I., Cooper, J. D., Desmond, S. S., Lunte, C. E., and Lunte, S. M. (2000) Analytical considerations for microdialysis sampling. *Adv. Drug Delivery Rev.* 45, 169–188.
- (3) Watson, C. J., Venton, B. J., and Kennedy, R. T. (2006) In Vivo Measurements of Neurotransmitters by Microdialysis Sampling. *Anal. Chem.* 78, 1391–1399.
- (4) Westerink, B. H., Cremers, T. I. F. H., Eds. (2007) *Handbook of Microdialysis: Methods, Applications and Perspectives*, Academic Press, London.
- (5) Yang, H., Thompson, A. B., McIntosh, B. J., Altieri, S. C., and Andrews, A. M. (2013) Physiologically Relevant Changes in Serotonin Resolved by Fast Microdialysis. *ACS Chem. Neurosci.* 4, 790–798.
- (6) Vander Weele, C. M., Porter-Stransky, K. A., Mabrouk, O. S., Lovic, V., Singer, B. F., Kennedy, R. T., and Aragona, B. J. (2014) Rapid dopamine transmission within the nucleus accumbens: dramatic difference between morphine and oxycodone delivery. *Eur. J. Neurosci.* 40, 3041–3054.
- (7) Gu, H., Varner, E. L., Groskreutz, S. R., Michael, A. C., and Weber, S. G. (2015) In Vivo Monitoring of Dopamine by Microdialysis with 1 min Temporal Resolution Using Online Capillary Liquid Chromatography with Electrochemical Detection. *Anal. Chem.* 87, 6088–6094.
- (8) Feuerstein, D., Manning, A., Hashemi, P., Bhatia, R., Fabricius, M., Toliás, C., Pahl, C., Ervine, M., Strong, A. J., and Boutelle, M. G. (2010) Dynamic metabolic response to multiple spreading depolarizations in patients with acute brain injury: an online microdialysis study. *J. Cereb. Blood Flow Metab.* 30, 1343–1355.
- (9) Benveniste, H., and Diemer, N. H. (1987) Cellular reactions to implantation of a microdialysis tube in the rat hippocampus. *Acta Neuropathol.* 74, 234–238.
- (10) Clapp-Lilly, K. L., Roberts, R. C., Duffy, L. K., Irons, K. P., Hu, Y., and Drew, K. L. (1999) An ultrastructural analysis of tissue surrounding a microdialysis probe. *J. Neurosci. Methods* 90, 129–142.
- (11) Zhou, F., Zhu, X., Castellani, R. J., Stimmelmayer, R., Perry, G., Smith, M. A., and Drew, K. L. (2001) Hibernation, a model of neuroprotection. *Am. J. Pathol.* 158, 2145–2151.
- (12) Hascup, E. R., af Bjerken, S., Hascup, K. N., Pomerleau, F., Huettl, P., Stromberg, I., and Gerhardt, G. A. (2009) Histological studies of the effects of chronic implantation of ceramic-based microelectrode arrays and microdialysis probes in rat prefrontal cortex. *Brain Res.* 1291, 12–20.
- (13) Jaquins-Gerstl, A., Shu, Z., Zhang, J., Liu, Y., Weber, S. G., and Michael, A. C. (2011) Effect of dexamethasone on gliosis, ischemia, and dopamine extraction during microdialysis sampling in brain tissue. *Anal. Chem.* 83, 7662–7667.
- (14) Nesbitt, K. M., Jaquins-Gerstl, A., Skoda, E. M., Wipf, P., and Michael, A. C. (2013) Pharmacological Mitigation of Tissue Damage during Brain Microdialysis. *Anal. Chem.* 85, 8173–8179.
- (15) Nesbitt, K. M., Varner, E. L., Jaquins-Gerstl, A., and Michael, A. C. (2015) Microdialysis in the Rat Striatum: Effects of 24 h Dexamethasone Retrodialysis on Evoked Dopamine Release and Penetration Injury. *ACS Chem. Neurosci.* 6, 163–173.
- (16) Groothuis, J., Ramsey, N. F., Ramakers, G. M., and van der Plasse, G. (2014) Physiological challenges for intracortical electrodes. *Brain Stimul.* 7, 1–6.
- (17) Zhong, Y., and Bellamkonda, R. V. (2007) Dexamethasone-coated neural probes elicit attenuated inflammatory response and neuronal loss compared to uncoated neural probes. *Brain Res.* 1148, 15–27.
- (18) Borland, L. M., Shi, G., Yang, H., and Michael, A. C. (2005) Voltammetric study of extracellular dopamine near microdialysis probes acutely implanted in the striatum of the anesthetized rat. *J. Neurosci. Methods* 146, 149–158.
- (19) Wang, Y., and Michael, A. C. (2012) Microdialysis probes alter presynaptic regulation of dopamine terminals in rat striatum. *J. Neurosci. Methods* 208, 34–39.
- (20) Robinson, T. E., and Camp, D. M. (1991) The effects of four days of continuous striatal microdialysis on indices of dopamine and serotonin neurotransmission in rats. *J. Neurosci. Methods* 40, 211–222.
- (21) Holson, R. R., Bowyer, J. F., Clausing, P., and Gough, B. (1996) Methamphetamine-stimulated striatal dopamine release declines rapidly over time following microdialysis probe insertion. *Brain Res.* 739, 301–307.
- (22) Holson, R. R., Gazzara, R. A., and Gough, B. (1998) Declines in stimulated striatal dopamine release over the first 32 h following microdialysis probe insertion: generalization across releasing mechanisms. *Brain Res.* 808, 182–189.
- (23) Yang, H., Michael, A. C. (2007) In Vivo Fast-Scan Cyclic Voltammetry of Dopamine near Microdialysis Probes, in *Electrochemical Methods for Neuroscience*, CRC Press, Boca Raton, FL.
- (24) Sharp, T., Ljungberg, T., Zetterstrom, T., and Ungerstedt, U. (1986) Intracerebral dialysis coupled to a novel activity box—a method to monitor dopamine release during behaviour. *Pharmacol., Biochem. Behav.* 24, 1755–1759.
- (25) Lu, Y., Peters, J. L., and Michael, A. C. (1998) Direct comparison of the response of voltammetry and microdialysis to electrically evoked release of striatal dopamine. *J. Neurochem.* 70, 584–593.
- (26) Yang, H., Peters, J. L., and Michael, A. C. (1998) Coupled effects of mass transfer and uptake kinetics on in vivo microdialysis of dopamine. *J. Neurochem.* 71, 684–692.
- (27) Bungay, P. M., Newton-Vinson, P., Isele, W., Garris, P. A., and Justice, J. B. (2003) Microdialysis of dopamine interpreted with quantitative model incorporating probe implantation trauma. *J. Neurochem.* 86, 932–946.
- (28) Floresco, S. B., West, A. R., Ash, B., Moore, H., and Grace, A. A. (2003) Afferent modulation of dopamine neuron firing differentially regulates tonic and phasic dopamine transmission. *Nat. Neurosci.* 6, 968–973.
- (29) Qian, J., Wu, Y., Yang, H., and Michael, A. C. (1999) An Integrated Decoupler for Capillary Electrophoresis with Electrochemical Detection: Application to Analysis of Brain Microdialysate. *Anal. Chem.* 71, 4486–4492.
- (30) Peters, J. L., and Michael, A. C. (1998) Modeling voltammetry and microdialysis of striatal extracellular dopamine: the impact of dopamine uptake on extraction and recovery ratios. *J. Neurochem.* 70, 594–603.
- (31) Yang, H., Peters, J. L., Allen, C., Chern, S. S., Coalson, R. D., and Michael, A. C. (2000) A theoretical description of microdialysis with mass transport coupled to chemical events. *Anal. Chem.* 72, 2042–2049.
- (32) Walters, S. H., Robbins, E. M., and Michael, A. C. (2015) Modeling the Kinetic Diversity of Dopamine in the Dorsal Striatum. *ACS Chem. Neurosci.* 6, 1468–1475.
- (33) Graeber, M. B., Streit, W. J., and Kreutzberg, G. W. (1989) Identity of ED2-positive perivascular cells in rat brain. *J. Neurosci. Res.* 22, 103–106.



(34) Ferrari, C. C., Depino, A. M., Prada, F., Muraro, N., Campbell, S., Podhajcer, O., Perry, V. H., Anthony, D. C., and Pitossi, F. J. (2004) Reversible demyelination, blood-brain barrier breakdown, and pronounced neutrophil recruitment induced by chronic IL-1 expression in the brain. *Am. J. Pathol.* 165, 1827–1837.

(35) Lecca, D., Cacciapaglia, F., Valentini, V., Acquas, E., and Di Chiara, G. (2007) Differential neurochemical and behavioral adaptation to cocaine after response contingent and noncontingent exposure in the rat. *Psychopharm.* 191, 653–667.

(36) Lecca, D., Cacciapaglia, F., Valentini, V., Gronli, J., Spiga, S., and Di Chiara, G. (2006) Preferential increase of extracellular dopamine in the rat nucleus accumbens shell as compared to that in the core during acquisition and maintenance of intravenous nicotine self-administration. *Psychopharm.* 184, 435–446.

(37) Bassareo, V., Cucca, F., Frau, R., and Di Chiara, G. (2015) Monitoring dopamine transmission in the rat nucleus accumbens shell and core during acquisition of nose-poking for sucrose. *Behav. Brain Res.* 287, 200–206.

(38) Dietrich, J., Rao, K., Pastorino, S., and Kesari, S. (2011) Corticosteroids in brain cancer patients: benefits and pitfalls. *Expert Rev. Clin. Pharmacol.* 4, 233–242.

(39) Iasevoli, F., Aloj, L., Latte, G., Avvisati, L., Marmo, F., Tomasetti, C., Buonaguro, E., Simeoli, C., Pivonello, R., Colao, A., and Bartolomeis, A. (2014) The Glucocorticoid Analog Dexamethasone Alters the Expression and the Distribution of Dopamine Receptors and Enkephalin within Cortico-Subcortical Regions. *Curr. Mol. Pharmacol.* 6, 149–155.

(40) Lammers, C. H., D'Souza, U. M., Qin, Z. H., Lee, S. H., Yajima, S., and Mouradian, M. M. (1999) Regulation of striatal dopamine receptors by corticosterone: an in vivo and in vitro study. *Mol. Brain Res.* 69, 281–285.

(41) Gasser, P. J., Lowry, C. A., and Orchinik, M. (2006) Corticosterone-sensitive monoamine transport in the rat dorsomedial hypothalamus: potential role for organic cation transporter 3 in stress-induced modulation of monoaminergic neurotransmission. *J. Neurosci.* 26, 8758–8766.

(42) Lindley, S. E., Bengoechea, T. G., Schatzberg, A. F., and Wong, D. L. (1999) Glucocorticoid effects on mesotelencephalic dopamine neurotransmission. *Neuropsychopharmacology* 21, 399–407.

(43) Lindley, S. E., Bengoechea, T. G., Wong, D. L., and Schatzberg, A. F. (2002) Mesotelencephalic dopamine neurochemical responses to glucocorticoid administration and adrenalectomy in Fischer 344 and Lewis rats. *Brain Res.* 958, 414–422.

(44) Paxinos, G., Watson, C. (1998) *The Rat Brain in Stereotaxic Coordinates*, 4<sup>th</sup> Edn, Academic Press, San Diego, CA.